I.V. STASYUK, V.O. KRASNOV

Institute for Condensed Matter Physics of the Nat. Acad. of Sci. of Ukraine
(1, Svientsitskii Str., Lviv 79011, Ukraine)

ENERGY SPECTRUM OF THE PSEUDOSPIN-ELECTRON MODEL IN A DYNAMICAL MEAN-FIELD APPROACH

The pseudospin-electron model in the case of infinite on-site electron repulsion is investigated. The electron energy spectrum is calculated within the framework of the dynamical mean field theory (DMFT), and the alloy analogy approximation is developed. The effect of the pseudospin-electron interaction, local asymmetry field, and tunneling-like level splitting on the existence and the number of electron subbands is investigated. The relation of the pseudospin-electron model to the problem of energy spectrum of boson-fermion mixtures in optical lattices is discussed.

K e y w o r d s: pseudospin-electron model, boson-fermion mixtures, dynamical mean field theory

1. Introduction

The pseudospin-electron model (PEM) is one of the models, which are used in the physics of strongly correlated electron systems in recent years. Application of the model to high-temperature superconductors allows one, for example, to describe the thermodynamics of an anharmonic oxygen ion subsystem and to explain the occurrence of inhomogeneous states and the bistability phenomena ([1], see also [2]). In this model, one considers the dynamics of locally anharmonic structure elements (using the pseudospin variables to describe them), interaction between pseudospins and electrons, and the asymmetry of local anharmonic potential wells. The electron subsystem is described by the Hubbard Hamiltonian.

In [3], a pseudospin-electron model of ion intercalation in crystals was formulated; the pseudospin representation is also used in the description of ionic conductors [4, 5]. The thermodynamics of the model has been investigated in the mean-field approximation; it was shown that a new phase with $\langle S^x \rangle \neq 0$ appears due to the ion hopping between sites. This new phase is an analogue of the superfluid phase in the systems of hard-core bosons or the superionic phase in ionic (protonic) conductors.

The pseudospin-electron model in its general form has also a direct relation to the ultra-cold boson-fermion mixtures in optical lattices, which are the object of an intense theoretical investigation during last years [6–10]. In the hard-core boson limit (that corresponds to the large on-site repulsion between Bose atoms), when the pseudospin representation is

used, one has to do with a pseudospin-fermion analogue of PEM [11]. The transverse field exists here in the phase with a Bose–Einstein (BE) condensate and is proportional to the order parameter $\langle S^x \rangle$, while the longitudinal field plays the role of a chemical potential of bosons. In this case, the investigation of the electron spectrum within PEM gives, at the same time, an information about the fermion spectrum of the boson-fermion system with $n_b \leq 1$ in the mentioned phase.

Investigations of the thermodynamics and the dynamics of PEM were performed mostly within the Hartree–Fock-type approximation (in the weak pseudospin-electron coupling case) or the generalized random phase approximation (at the strong coupling); the problem is reviewed and discussed in [2]. The conditions of the appearance of modulated phases, phase transitions between different uniform phases, and phase separation were established.

In the DMFT approach, the Hamiltonian with strong correlations is taken in the infinite space dimension $(d \rightarrow \infty)$ limit; this leads to a reformulation of the problem and the transition to the solution of the single-site problem described by an effective Hamiltonian [12–14]. Only for simplest cases such as mobile particles in the Falicov–Kimball model, one can solve analytically this problem. An exact solution exists also for the pseudospin-electron model without transverse field [15]. There are also some approximate analytical approaches such as: Hubbard-I, Hubbard-III, alloy analogy (AA), modified alloy analogy (MAA) *etc.*, see [16, 17].

In this work, the alloy analogy approximation for the single-site problem is used within the pseudospin-

electron model. Our problem is solved in the limit of infinite value of single-site electron interaction. The previous consideration of this problem in the Hubbard-I approximation [18] revealed a complicated structure of the spectrum and the presence of some number of subbands. In [19], the electron energy spectrum of the pseudospin-electron model allowing the interaction of near-energy subbands was considered. The effective single-site problem was solved within the auxiliary fermion field approach with the help of the procedure of different-time decoupling of higher order Green's functions [16].

Our main task is to investigate a reconstruction of the electron energy spectrum and to describe the effect of band splitting at a change of the longitudinal and transverse fields and the pseudospin-electron interaction constant.

2. Hamiltonian of the Model and its Transformation

The Hamiltonian of the pseudospin-electron model is

$$H = \sum_i H_i + \sum_{<i,j>,\sigma} t_{ij} c_{i\sigma}^+ c_{j\sigma}, \qquad (1)$$

where Ω in the single-site part of the Hamiltonian is the tunneling-like level splitting, g is the pseudospin-electron interaction constant, and h is the asymmetry of the local anharmonic potential:

$$H_i = -\mu(n_{i,\uparrow}+n_{i,\downarrow})+g(n_{i,\uparrow}+n_{i,\downarrow})S_i^z-\Omega S_i^x-hS_i^z. \quad (2)$$

The second term in (1) describes the electron site-to-site hopping (between nearest neighbours).

The term $Un_\uparrow n_\downarrow$ is not included, as we investigate our problem in the limit of the infinite potential of single-site electron interaction $U \to \infty$, where all states with double cite occupation are absent. The single-site Hamiltonian is considered as the zero-order one with respect to the electron transfer. It is useful to introduce the standard single-site basis $|R\rangle = |n_{i,\uparrow}, n_{i,\downarrow}, S_i^z\rangle$, with six eigenvectors [18]:

$$|1\rangle = \left|0,0,\frac{1}{2}\right\rangle, \quad |3\rangle = \left|0,1,\frac{1}{2}\right\rangle, \quad |4\rangle = \left|1,0,\frac{1}{2}\right\rangle,$$

$$|\widetilde{1}\rangle = \left|0,0,-\frac{1}{2}\right\rangle, \quad |\widetilde{3}\rangle = \left|0,1,-\frac{1}{2}\right\rangle, \quad |\widetilde{4}\rangle = \left|1,0,-\frac{1}{2}\right\rangle. \tag{3}$$

Using Hubbard X-operators that act in the space of such eigenvectors, we can write down the electron

annihilation (creation) operators and the pseudospin operators (in the limit, when the state $|2\rangle = |1,1,\pm\frac{1}{2}\rangle$ is unoccupied) as follows: [18]

$$c_{i,\uparrow} = \mathrm{X}_i^{14} + \mathrm{X}_i^{\widetilde{14}},$$

$$c_{i,\downarrow} = \mathrm{X}_i^{13} + \mathrm{X}_i^{\widetilde{13}} \tag{4}$$

Then, the single-site part of the Hamiltonian can be expressed by means of X-operators in the following way:

$$H_i = (-\mu + \frac{g}{2} - \frac{h}{2})(\mathrm{X}_i^{33} + \mathrm{X}_i^{44})+$$

$$+(-\mu - \frac{g}{2} + \frac{h}{2})(\mathrm{X}_i^{\widetilde{33}} + \mathrm{X}_i^{\widetilde{44}}) + \frac{h}{2}(\mathrm{X}_i^{\widetilde{11}} - \mathrm{X}_i^{11})+$$

$$+\frac{\Omega}{2}(\mathrm{X}_i^{1\widetilde{1}} + \mathrm{X}_i^{\widetilde{11}} + \mathrm{X}_i^{3\widetilde{3}} + \mathrm{X}_i^{\widetilde{33}} + \mathrm{X}_i^{4\widetilde{4}} + \mathrm{X}_i^{\widetilde{44}}). \tag{5}$$

This Hamiltonian is diagonal in the case $\Omega = 0$. But if the tunneling splitting is non-zero, we have to use a transformation

$$\begin{pmatrix} R \\ \widetilde{R} \end{pmatrix} = \begin{pmatrix} \cos\phi_r & \sin\phi_r \\ -\sin\phi_r & \cos\phi_r \end{pmatrix} \begin{pmatrix} r \\ \widetilde{r} \end{pmatrix} \tag{6}$$

to diagonalize it. Here,

$$\cos(2\phi_r) = \frac{n_r g - h}{\sqrt{(n_r g - h)^2 + \Omega^2}},$$

$$n_1 = 0, n_3 = n_4 = 1. \tag{7}$$

In that way, we have

$$H = \sum_{i,r} \varepsilon_r X_i^{rr} + \sum_{<i,j>,\sigma} t_{ij} c_{i\sigma}^+ c_{j\sigma},$$

$$\varepsilon_{1,\widetilde{1}} = \pm\frac{1}{2}\sqrt{h^2 + \Omega^2},$$

$$\varepsilon_{3,\widetilde{3}} = \varepsilon_{4,\widetilde{4}} = -\mu \pm \frac{1}{2}\sqrt{(g-h)^2 + \Omega^2}. \tag{8}$$

Here, making transformation (6), we obtain

$$c_{i,\uparrow} = \cos\phi_{41}(X_i^{14} + X_i^{\widetilde{14}}) + \sin\phi_{41}(X_i^{1\widetilde{4}} - X_i^{\widetilde{14}}),$$

$$c_{i,\downarrow} = \cos\phi_{31}(X_i^{13} + X_i^{\widetilde{13}}) + \sin\phi_{31}(X_i^{1\widetilde{3}} - X_i^{\widetilde{13}}),$$

$$\cos\phi_{41} = \cos(\phi_4 - \phi_1), \quad \cos\phi_{31} = \cos(\phi_3 - \phi_1),$$

$$\sin\phi_{41} = \sin(\phi_4 - \phi_1), \quad \sin\phi_{31} = \sin(\phi_3 - \phi_1). \tag{9}$$

where X-operators act on the new basis.

3. Dynamical Mean Field Theory Approach

The transition to the $d = \infty$ limit in the DMFT approach is accompanied by the scaling of the electron transfer parameter:

$$t_{ij} \rightarrow \frac{t_{ij}}{\sqrt{d}}. \tag{10}$$

In particular, the self-energy part of electron Green's function becomes purely local [13, 14]:

$$\Sigma_{ij,\sigma}(\omega) = \Sigma_\sigma \delta_{ij}, \qquad d = \infty. \tag{11}$$

The Fourier-transform $\Sigma_{ij,\sigma}(\omega)$ is, hence, momentum-independent:

$$\Sigma_\sigma(\mathbf{k}, \omega) = \Sigma_\sigma(\omega). \tag{12}$$

Electron Green's function in the (k, ω) representation

$$G_k^\sigma(\omega) = \sum_{i-j} e^{i\mathbf{k}(\mathbf{R}_i - \mathbf{R}_j)} G_{ij,\sigma}(\omega) \tag{13}$$

can be expressed as

$$G_k^\sigma(\omega) = \frac{1}{[\Xi_\sigma(\omega)]^{-1} - t_k}, \tag{14}$$

where $\Xi_\sigma(\omega)$ is the part, which is irreducible (in the diagrammatic representation) according to Larkin. To calculate the $\Xi_\sigma(\omega)$ function, the effective single-site problem is used. The transition to this problem corresponds to the replacement

$$e^{-\beta H} \rightarrow e^{-\beta H_{\text{eff}}} = e^{-\beta H_0} T \exp\Big\{ - \int\limits_0^\beta d\tau \times$$

$$\times \int\limits_0^\beta d\tau' \sum_\sigma J_\sigma(\tau - \tau') a_\sigma^+(\tau) a_\sigma(\tau') \Big\} \equiv e^{-\beta H_0} \widetilde{\sigma}(\beta), \tag{15}$$

where

$$H_0 = H_i, \tag{16}$$

and $J_\sigma(\tau - \tau')$ is an effective time-dependent field (coherent potential) that is determined self-consistently from the condition that the same self-energy part $\Xi_\sigma(\omega)$ determines the lattice function $G_k^\sigma(\omega)$, as well as the Green's function $G_\sigma^{(a)}(\omega)$ of the effective single-site problem:

$$G_\sigma^{(a)}(\omega) = \frac{1}{[\Xi_\sigma(\omega)]^{-1} - J_\sigma(\omega)}. \tag{17}$$

In this case, we have

$$G_\sigma^{(a)} = G_{ii,\sigma}(\omega) = \frac{1}{N} \sum_k G_k^\sigma(\omega). \tag{18}$$

The system of simultaneous equations (14), (17), and (18) becomes closed, when it is supplemented with the functional dependence

$$G_\sigma^{(a)}(\omega) = f([J_\sigma(\omega)]), \tag{19}$$

which is obtained as a result of solving the effective single-site problem with the statistical operator $\exp(-\beta H_{\text{eff}})$.

4. Reformulation of Wick's Theorem for the Single-Site Problem

To find out relation (19), let us calculate electron Green's function using an expansion in powers of the coherent potential $J_\sigma(\omega)$. In the zero approximation:

$$-\langle T X^{qp}(\tau) X^{pq}(\tau') \rangle_0 = -g_0^{qp}(\tau - \tau') \langle X^{qq} + X^{pp} \rangle_0. \tag{20}$$

In the frequency representation: $g_0^{qp}(\omega_n) = -(i\omega_n - \lambda_{pq})^{-1}$, $\lambda_{pq} = \varepsilon_p - \varepsilon_q$.

Using Wick's theorem for the Hubbard operators [20], we can see that

$$\overset{\frown}{X^{41}(\tau') X^{14}}(\tau) = -g_0^{14}(\tau - \tau')(X^{11} + X^{44})_{\tau'}$$

$$\overset{\frown}{X^{\widetilde{41}}(\tau') X^{14}}(\tau) = 0$$

$$\overset{\frown}{X^{\widetilde{41}}(\tau') X^{14}}(\tau) = -g_0^{14}(\tau - \tau') X^{\widetilde{44}}(\tau')$$

$$\overset{\frown}{X^{4\widetilde{1}}(\tau') X^{14}}(\tau) = -g_0^{14}(\tau - \tau') X^{1\widetilde{1}}(\tau')$$

As a result of such a procedure, the Bose-type X-operators appear.

The alloy analogy approximation (see [16, 17]) means the neglect of all non-diagonal Hubbard operators in Wick's pairings. Such an approximation leads to the next result:

$$\overset{\frown}{c_\uparrow^+(\tau') X^{14}}(\tau) = -g_0^{14}(\tau - \tau')(X^{11} + X^{44})_{\tau'} \cos\phi_{41},$$

$$\overset{\frown}{c_\downarrow^+(\tau') X^{14}}(\tau) = 0,$$

$$\overset{\frown}{c_\uparrow^+(\tau') X^{\widetilde{14}}}(\tau) = -g_0^{\widetilde{14}}(\tau - \tau')(X^{\widetilde{11}} + X^{\widetilde{44}})_{\tau'} \cos\phi_{41},$$

$$\overset{\longleftrightarrow}{c_\downarrow^+(\tau')X^{\widetilde{14}}(\tau)} = 0,$$

$$\overset{\longleftrightarrow}{c_\uparrow^+(\tau')X^{\widetilde{14}}(\tau)} = g_0^{\widetilde{14}}(\tau - \tau')(X^{\widetilde{11}} + X^{44})_{\tau'} \sin\phi_{41},$$

$$\overset{\longleftrightarrow}{c_\downarrow^+(\tau')X^{1\widetilde{4}}(\tau)} = 0,$$

$$\overset{\longleftrightarrow}{c_\uparrow^+(\tau')X^{1\widetilde{4}}(\tau)} = -g_0^{1\widetilde{4}}(\tau - \tau')(X^{11} + X^{\widetilde{44}})_{\tau'} \sin\phi_{41},$$

$$\overset{\longleftrightarrow}{c_\downarrow^+(\tau')X^{1\widetilde{4}}(\tau)} = 0. \tag{21}$$

Using (9), we have

$$\overset{\longleftrightarrow}{c_\uparrow^+(\tau')c_\uparrow(\tau)} = -g_0^{14}(\tau - \tau')(X^{11} + X^{44})_{\tau'} \cos^2\phi_{41} -$$

$$-g_0^{\widetilde{14}}(\tau - \tau')(X^{\widetilde{11}} + X^{\widetilde{44}})_{\tau'} \cos^2\phi_{41} -$$

$$-g_0^{\widetilde{14}}(\tau - \tau')(X^{\widetilde{11}} + X^{44})_{\tau'} \sin^2\phi_{41} -$$

$$-g_0^{1\widetilde{4}}(\tau - \tau')(X^{11} + X^{\widetilde{44}})_{\tau'} \sin^2\phi_{41}. \tag{22}$$

This result shows us that, in the case of the alloy analogy approximation the pairing of Fermi-operators decomposes into the sum of terms that are the projections on single-site states (because of the action of X^{rr} operators). This is the main difference from the case of ideal fermions, where we have Green's functions as a result of the pairing.

Now, we can rewrite

$$\overset{\longleftrightarrow}{c_\uparrow^+(\tau')c_\uparrow(\tau)} =$$

$$-[g_0^{14}(\tau-\tau')\cos^2\phi_{41} + g_0^{1\widetilde{4}}(\tau-\tau')\sin\phi_{41}]X^{11}(\tau') -$$

$$-[g_0^{\widetilde{14}}(\tau-\tau')\cos^2\phi_{41} + g_0^{14}(\tau-\tau')(\sin\phi_{41}]X^{\widetilde{11}}(\tau') -$$

$$-[g_0^{14}(\tau-\tau')\cos^2\phi_{41} + g_0^{1\widetilde{4}}(\tau-\tau')\sin\phi_{41}]X^{44}(\tau') -$$

$$-[g_0^{\widetilde{14}}(\tau-\tau')\cos^2\phi_{41} + g_0^{1\widetilde{44}}(\tau-\tau')\sin\phi_{41}]X^{\widetilde{44}}(\tau') \equiv$$

$$-g_{0\uparrow}^{(1)}X^{11}(\tau') - g_{0\uparrow}^{(\widetilde{1})}X^{\widetilde{11}}(\tau') - g_{0\uparrow}^{(4)}X^{44}(\tau') -$$

$$-g_{0\uparrow}^{(\widetilde{4})}X^{\widetilde{44}}(\tau') = -\sum_r g_{0\uparrow}^{(r)}X^{rr}(\tau'). \tag{23}$$

5. Single-Site Green's Function

In general, electron Green's function of the effective one-site problem reads

$$\Upsilon_\sigma(\tau - \tau') = -\frac{\langle Tc_\sigma(\tau)c_\sigma^+(\tau')e^{-\beta H_{\text{eff}}}\rangle}{\langle e^{-\beta H_{\text{eff}}}\rangle} =$$

$$= -\frac{\langle Tc_\sigma(\tau)c_\sigma^+(\tau')\widetilde{\sigma}(\beta)\rangle_0}{\langle \widetilde{\sigma}(\beta)\rangle_0}. \tag{24}$$

The numerator and denominator in this expression will be calculated separately using an expansion in terms of the coherent potential $J_\sigma(\tau-\tau')$. As the first step, we illustrate the second order in this expansion with four operators of creation and annihilation of electrons:

$$\langle Tc_\uparrow(\tau)c_\uparrow^+(\tau')c_\uparrow^+(\tau_1)c_\uparrow(\tau_2)\rangle_0 =$$

$$= \langle T\overset{\longleftrightarrow}{c_\uparrow^+(\tau)c_\uparrow(\tau)}\overset{\longleftrightarrow}{c_\uparrow^+(\tau_1)c_\uparrow(\tau_2)}\rangle_0 +$$

$$+\langle T\overset{\longleftrightarrow}{c_\uparrow^+(\tau_1)c_\uparrow(\tau)}\overset{\longleftrightarrow}{c_\uparrow^+(\tau')c_\uparrow(\tau_2)}\rangle_0 =$$

$$= -\sum_r g_{0\uparrow}^{(r)}(\tau - \tau')g_{0\uparrow}^{(r)}(\tau_2 - \tau_1)\langle X^{rr}\rangle_0 +$$

$$+\sum_r g_{0\uparrow}^{(r)}(\tau - \tau_1)g_{0\uparrow}^{(r)}(\tau_2 - \tau')\langle X^{rr}\rangle_0 \tag{25}$$

and

$$\langle Tc_\uparrow(\tau)c_\uparrow^+(\tau')c_\uparrow^+(\tau_1)c_\downarrow(\tau_2)\rangle_0 =$$

$$= -\langle T\overset{\longleftrightarrow}{c_\uparrow^+(\tau')c_\uparrow(\tau)}\overset{\longleftrightarrow}{c_\downarrow^+(\tau_1)c_\downarrow(\tau_2)}\rangle_0 =$$

$$= -\sum_r g_{0\uparrow}^{(r)}(\tau - \tau')g_{0\downarrow}^{(r)}(\tau_2 - \tau_1)\langle X^{rr}\rangle_0. \tag{26}$$

Here, the pairing of Fermi-operators is performed according to (25). The diagonal X-operators, which appear during this procedure, we multiply, by using the rule $X^{rr}X^{pp} = X^{rr}\delta_{rp}$. As a result, only the averages $\langle X^{rr}\rangle_0$ are present.

We can also consider the third order in our expansion with six operators of creation and annihilation of electrons:

$$\langle Tc_\uparrow(\tau)c_\uparrow^+(\tau')c_\uparrow^+(\tau_1)c_\uparrow(\tau_2)c_\uparrow^+(\tau_3)c_\uparrow(\tau_4)\rangle_0 =$$

$$= -\langle T\overset{\longleftrightarrow}{c_\uparrow^+(\tau')c_\uparrow(\tau)}c_\uparrow^+(\tau_1)c_\uparrow(\tau_2)c_\uparrow^+(\tau_3)c_\uparrow(\tau_4)\rangle_0 +$$

$$+\langle Tc_\uparrow^+(\tau')\overset{\longleftrightarrow}{c_\uparrow^+(\tau1)c_\uparrow(\tau)}c_\uparrow(\tau_2)c_\uparrow^+(\tau_3)c_\uparrow(\tau_4)\rangle_0 +$$

$$+\langle Tc_\uparrow^+(\tau')c_\uparrow^+(\tau_1)c_\uparrow(\tau_2)\rangle_0 c_\uparrow^+(\tau_3)c_\uparrow(\tau)c_\uparrow(\tau_4)\rangle_0 =$$

$$= -\langle Tc_\uparrow^+(\tau')c_\uparrow(\tau)c_\uparrow^+(\tau_1)c_\uparrow(\tau_2)c_\uparrow^+(\tau_3)c_\uparrow(\tau_4)\rangle_0 +$$

$$+\langle Tc_\uparrow^+(\tau')c_\uparrow(\tau)c_\uparrow^+(\tau_1)c_\uparrow(\tau_4)c_\uparrow^+(\tau_3)c_\uparrow(\tau_2)\rangle_0 +$$

$$c_\uparrow(\tau_2)c_\uparrow^+(\tau_1)c_\uparrow(\tau)c_\uparrow^+(\tau_3)c_\uparrow(\tau_4)\rangle_0 -$$

$$-\langle Tc_\uparrow^+(\tau')c_\uparrow(\tau_4)c_\uparrow^+(\tau_1)c_\uparrow(\tau)c_\uparrow^+(\tau_3)c_\uparrow(\tau_2)\rangle_0 +$$

$$+\langle Tc_\uparrow^+(\tau')c_\uparrow(\tau_4)c_\uparrow^+(\tau_1)c_\uparrow(\tau_2)c_\uparrow^+(\tau_3)c_\uparrow(\tau)\rangle_0 -$$

$$-\langle Tc_\uparrow^+(\tau')c_\uparrow(\tau_2)c_\uparrow^+(\tau_3)c_\uparrow(\tau)c_\uparrow^+(\tau_1)c_\uparrow(\tau_4)\rangle_0. \quad (27)$$

Finally,

$$\langle Tc_\uparrow(\tau)c_\uparrow^+(\tau')c_\uparrow^+(\tau_1)c_\uparrow(\tau_2)c_\uparrow^+(\tau_3)c_\uparrow(\tau_4)\rangle_0 =$$

$$= \sum_r g_{0\uparrow}^{(r)}(\tau-\tau')g_{0\uparrow}^{(r)}(\tau_2-\tau_1)g_{0\uparrow}^{(r)}(\tau_4-\tau_3)\langle X^{rr}\rangle_0 -$$

$$- \sum_r g_{0\uparrow}^{(r)}(\tau-\tau')g_{0\uparrow}^{(r)}(\tau_4-\tau_1)g_{0\uparrow}^{(r)}(\tau_2-\tau_3)\langle X^{rr}\rangle_0 -$$

$$- \sum_r g_{0\uparrow}^{(r)}(\tau_2-\tau')g_{0\uparrow}^{(r)}(\tau-\tau_1)g_{0\uparrow}^{(r)}(\tau_4-\tau_3)\langle X^{rr}\rangle_0 +$$

$$+ \sum_r g_{0\uparrow}^{(r)}(\tau_4-\tau')g_{0\uparrow}^{(r)}(\tau-\tau_1)g_{0\uparrow}^{(r)}(\tau_2-\tau_3)\langle X^{rr}\rangle_0 -$$

$$- \sum_r g_{0\uparrow}^{(r)}(\tau_4-\tau')g_{0\uparrow}^{(r)}(\tau_2-\tau_1)g_{0\uparrow}^{(r)}(\tau-\tau_3)\langle X^{rr}\rangle_0 +$$

$$+ \sum_r g_{0\uparrow}^{(r)}(\tau_2-\tau')g_{0\uparrow}^{(r)}(\tau-\tau_3)g_{0\uparrow}^{(r)}(\tau_4-\tau_1)\langle X^{rr}\rangle_0. \quad (28)$$

The similar procedure is also actual in the case of higher order terms. Using the diagrammatic series, we can separate the connected and disconnected "vacuum" (without external vertices) parts of diagrams. The former form a geometric progression in the frequency representation. The latter look like closed rings of different lengths (created by unperturbed Green's function and coherent potential lines) and give exponential contributions in subspaces $|r\rangle$ after the summation of infinite series.

So, the numerator in Green's function $\langle Tc_\uparrow(\tau)c_\uparrow^+(\tau')\rangle_{\text{num}}$ reads

$$\langle Tc_\uparrow(\tau)c_\uparrow^+(\tau')\rangle_{\text{num}} =$$

$$= \sum_r \Big[g_{0\uparrow}^{(r)}(\omega_n) - g_{0\uparrow}^{(r)}(\omega_n)J_\uparrow(\omega_n)g_{0\uparrow}^{(r)}(\omega_n) +$$

$$+ g_{0\uparrow}^{(r)}(\omega_n)J_\uparrow(\omega_n)g_{0\uparrow}^{(r)}(\omega_n)J_\uparrow(\omega_n)g_{0\uparrow}^{(r)}(\omega_n) -$$

$$- \dots \Big]\langle X^{rr}\rangle_0 e^{Q_r} = \sum_r \frac{g_{0\uparrow}^{(r)}(\omega_n)}{1+g_{0\uparrow}^{(r)}(\omega_n)J_\uparrow(\omega_n)}\langle X^{rr}\rangle_0 e^{Q_r}. \quad (29)$$

Here, Q_r in the analytical form is

$$Q_r = \sum_{\omega_n}\sum_\sigma g_{0\sigma}^{(r)}(\omega_n)J_\sigma(\omega_n) -$$

$$- \frac{1}{2}\Big[\sum_{\omega_n}\sum_\sigma g_{0\sigma}^{(r)}(\omega_n)J_\sigma(\omega_n)\Big]^2 +$$

$$+ \frac{1}{3}\Big[\sum_{\omega_n}\sum_\sigma g_{0\sigma}^{(r)}(\omega_n)J_\sigma(\omega_n)\Big]^3 - \dots =$$

$$= \sum_{\omega_n}\sum_\sigma \ln(1+g_{0\sigma}^{(r)}(\omega_n)J_\sigma(\omega_n)). \quad (30)$$

In particular,

$$Q_{1,\tilde{1}} = \sum_{\omega_n}\ln(1+g_{0\uparrow}^{(1,\tilde{1})}(\omega_n)J_\uparrow(\omega_n)) +$$

$$+ \sum_{\omega_n}\ln(1+g_{0\downarrow}^{(1,\tilde{1})}(\omega_n)J_\downarrow(\omega_n)),$$

$$Q_{3,\tilde{3}} = \sum_{\omega_n}\ln(1+g_{0\downarrow}^{(3,\tilde{3})}(\omega_n)J_\downarrow(\omega_n)),$$

$$Q_{4,\tilde{4}} = \sum_{\omega_n}\ln(1+g_{0\uparrow}^{(4,\tilde{4})}(\omega_n)J_\uparrow(\omega_n)). \quad (31)$$

The next step is to calculate the denominator

$$\langle\widetilde{\sigma}(\beta)\rangle_0 = 1 - \int_0^\beta d\tau_1 \int_0^\beta d\tau_2 \sum_\sigma J_\sigma(\tau_1-\tau_2)\times$$

$$\times\langle Tc_\sigma^+(\tau_1)c_\sigma(\tau_2)\rangle_0 + \frac{1}{2!}\int_0^\beta d\tau_1 \dots \int_0^\beta d\tau_4\times$$

$$\times\sum_\sigma\sum_{\sigma'} J_\sigma(\tau_1-\tau_2)J_{\sigma'}(\tau_3-\tau_4)\times$$

$$\times\langle Tc_\sigma^+(\tau_1)c_\sigma(\tau_2)c_{\sigma'}^+(\tau_3)c_{\sigma'}(\tau_4)\rangle_0 - \dots \quad (32)$$

In the diagrammatic representation, this series is expressed through the set of "vacuum" diagrams. The final result could be expressed in terms of contributions Q_r of the above-mentioned ring diagrams.
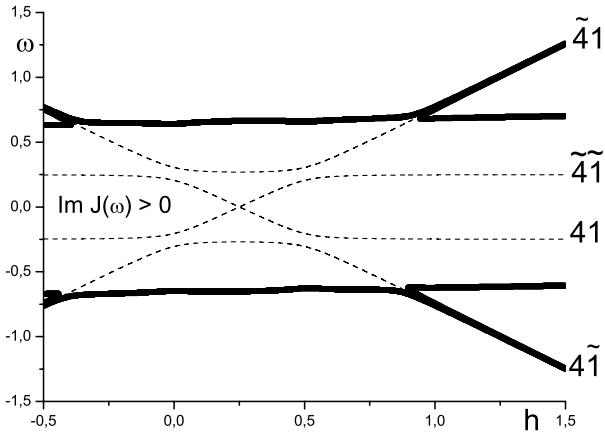
Fig. 1. Dependence of electron band boundaries on the asymmetry of the local anharmonic potential h ($g = 0.5$, $\Omega = 0.1$, $T = 0.02$, $\mu = 0$, $W = 0.5$). Hereinafter, dashed lines represent the energies of the transitions between single-site electron levels $pq = \lambda_{pq} = \varepsilon_p - \varepsilon_q$ without hopping

In such a case, we have

$$\langle \sigma(\beta) \rangle_0 = 1 + \sum_r \left[Q_r + \frac{1}{2!}Q_r^2 + \frac{1}{3!}Q_r^3 + \right.$$
$$\left. + \dots \right] \langle X^{rr} \rangle_0 = \sum_r e^{Q_r} \langle X^{rr} \rangle_0. \tag{33}$$

Finally, our analytical result is

$$\langle T c_\sigma^+ c_\sigma \rangle = \frac{\sum_r \frac{g_{0\sigma}^{(r)}(\omega_n)}{1 + g_{0\sigma}^{(r)}(\omega_n) J_\sigma(\omega_n)} \langle X^{rr} \rangle_0 e^{Q_r}}{\sum_p e^{Q_p} \langle X^{pp} \rangle_0}, \tag{34}$$

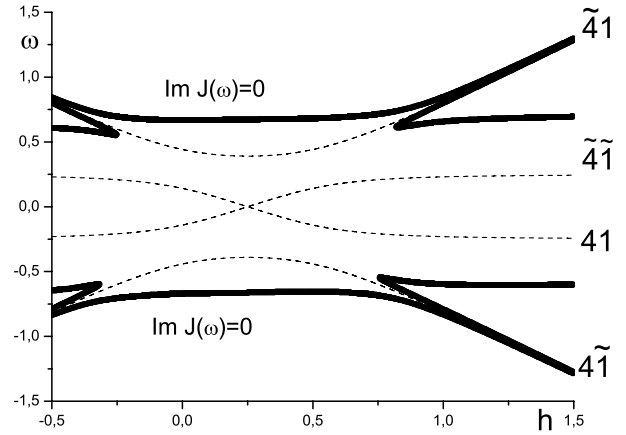where $\sigma = \uparrow$ or $\downarrow$.

6. Electron Energy Spectrum

Now, we have the closed system of equations to calculate Green's function $G_\uparrow^{(a)}(\omega)$ and the coherent potential $J_\uparrow(\omega)$:

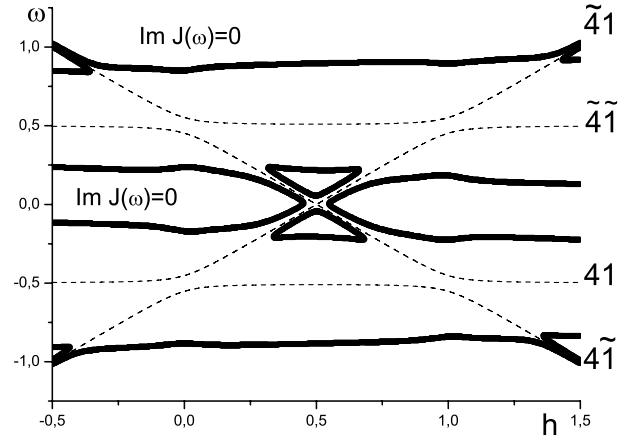$$G_k^\sigma(\omega) = \frac{1}{[\Xi_\sigma(\omega)]^{-1} - t_k},$$

$$G_\sigma^{(a)}(\omega) = \frac{1}{[\Xi_\sigma(\omega)]^{-1} - J_\sigma(\omega)} = \frac{1}{N}\sum_k G_k^\sigma(\omega),$$

$$G_\sigma^{(a)}(\omega) = \frac{\sum_r \frac{g_{0\sigma}^{(r)}(\omega_n)}{1 + g_{0\sigma}^{(r)}(\omega_n) J_\sigma(\omega_n)} \langle X^{rr} \rangle_0 e^{Q_r}}{\sum_p e^{Q_p} \langle X^{pp} \rangle_0},$$

$$Q_r = \sum_{\omega_n} \sum_\sigma \ln(1 + g_{0\sigma}^{(r)}(\omega_n) J_\sigma(\omega_n)). \tag{35}$$

Fig. 2. Dependence of electron band boundaries on the asymmetry of the local anharmonic potential h ($g = 0.5$, $\Omega = 0.3$, $T = 0.02$, $\mu = 0$, $W = 0.5$)
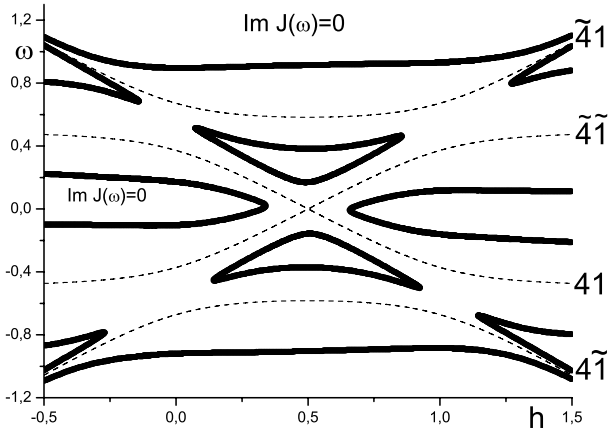

Fig. 3. Dependence of electron band boundaries on the asymmetry of the local anharmonic potential h ($g = 1.0$, $\Omega = 0.1$, $T = 0.02$, $\mu = 0$, $W = 0.5$)

Here, to calculate $\langle X^{rr} \rangle_0$, we use the iterative process: the next $\langle X^{rr} \rangle_0$ value depends on the previous $\langle X^{rr} \rangle_0'$ one as
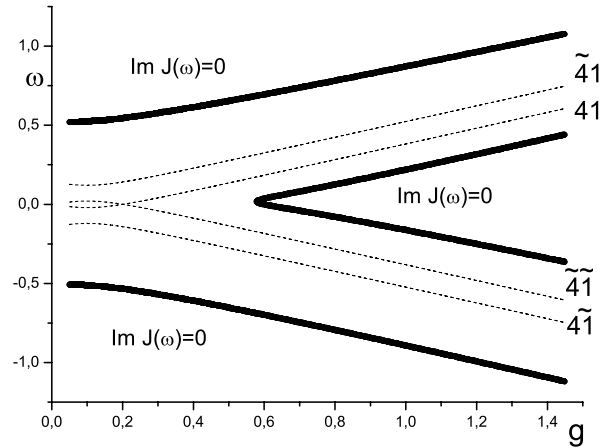
$$\langle X^{rr} \rangle_0 = \frac{\langle X^{rr} \rangle_0' e^{Q_r}}{\sum_{p=1,\tilde{1},4,\tilde{4}} \langle X^{pp} \rangle_0 e^{Q_p}}.$$

The initial averages are taken from the Boltzmann distribution $\langle X^{rr} \rangle_0 = \frac{e^{-\beta \varepsilon_r}}{\sum_p e^{-\beta \varepsilon_p}}$.

To sum over $\mathbf{k}$, we use the semielliptic density of states $\rho_0(t) = \frac{2}{\pi W^2}\sqrt{W^2 - t^2}$. In this case, $J_\sigma(\omega) = \frac{W^2}{4} G_\sigma^{(a)}(\omega)$ [12], and our final equation for the coher-

Fig. 4. Dependence of electron band boundaries on the asymmetry of the local anharmonic potential h ($g = 1.0$, $\Omega = 0.3$, $T = 0.02$, $\mu = 0$, $W = 0.5$)

Fig. 6. Dependence of electron band boundaries on the pseudospin-electron interaction constant g ($h = 1.0$, $\Omega = 0.3$, $T = 0.02$, $\mu = 0$, $W = 0.5$)

Fig. 5. Dependence of electron band boundaries on the pseudospin-electron interaction constant g ($h = 0.1$, $\Omega = 0.1$, $T = 0.02$, $\mu = 0$, $W = 0.5$)

Fig. 7. Dependence of electron band boundaries on the tunneling-like level splitting Ω ($g = 1.0$, $h = 0.1$, $T = 0.02$, $\mu = 0$, $W = 0.5$)
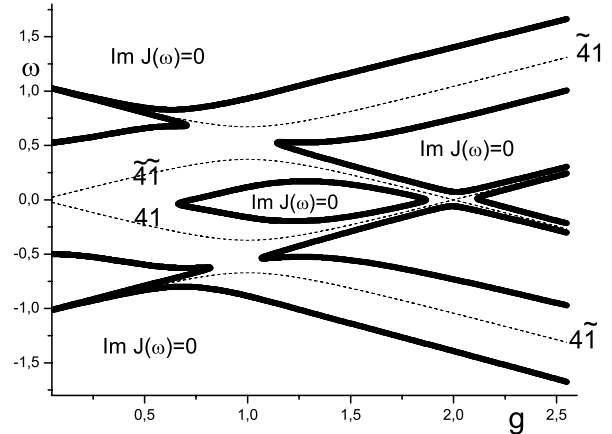
ent potential $J_\sigma(\omega)$ is as follows:

$$J_\sigma(\omega_n) = \frac{W^2}{4} \frac{\sum_r \frac{g_{0\sigma}^{(r)}(\omega_n)}{1 + g_{0\sigma}^{(r)}(\omega_n) J_\sigma(\omega_n)} \langle X^{rr} \rangle_0 e^{Q_r}}{\sum_p e^{Q_p} \langle X^{pp} \rangle_0}. \qquad (36)$$
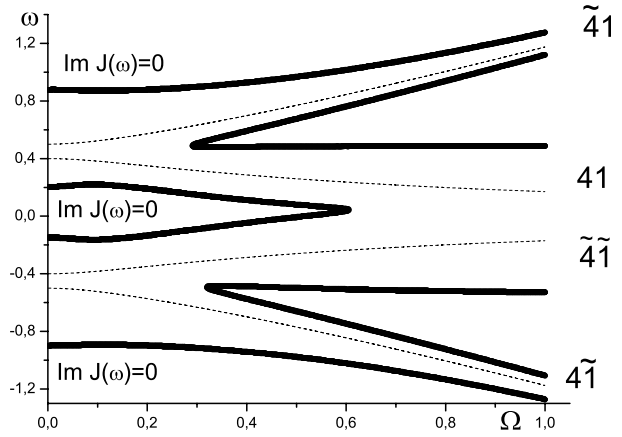
In a usual way, we perform the analytical continuation on the real axis ($i\omega_n \to \omega - i\delta$), and only the solutions with $\Im J_\sigma(\omega) > 0$ must be considered.

Electron band boundaries are determined from the condition $\Im J_\sigma(\omega) \to 0$. Their dependences on the asymmetry of the local anharmonic potential are shown in Figs. 1–4.

One can see the effect of the tunneling-like level splitting Ω on the width of existing bands (we can

compare the plots with constant $g = 0.5$ and to see that the increase of Ω from 0.1 to 0.3 leads to a noticable broadening of bands).

One can see also how the pseudospin-electron interaction g leads to the appearance of two additional bands, when $h \approx \frac{g}{2}$, and one band otherwise (this can be seen with comparing the plots with different g, but with the same Ω). The dependences of electron band boundaries on the pseudospin-electron interaction constant g are shown in Figs. 5–6. One can see that there exists some critical $g \approx W$, at which the additional gap appears in the spectrum. This result is similar to the Mott transition type reconstruction obtained in [15] for the pseudospin-electron model without tunneling-like level splitting.
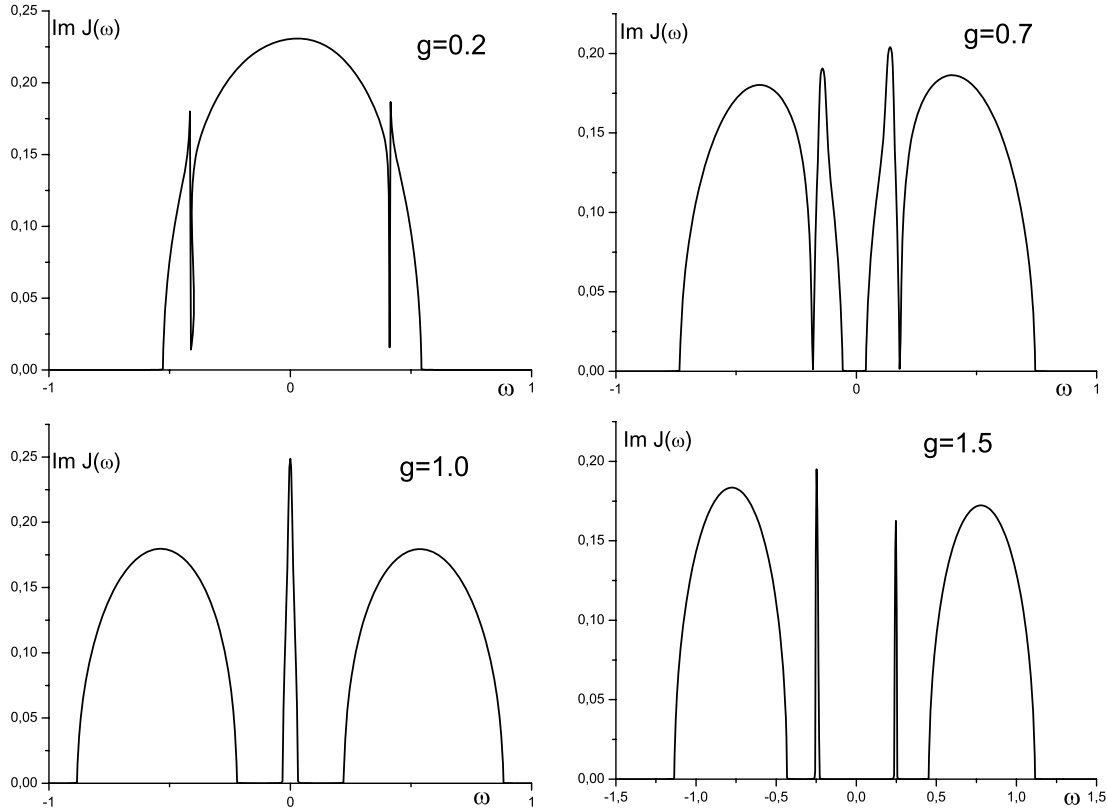
Fig. 8. Electron density of states at different values of the pseudospin-electron interaction constant g ($T = 0.02$, $\mu = 0$, $W = 0.5$)

Similarly to the dependence of the local anharmonic potential on the asymmetry, we can see also how an increase of Ω leads to the band width growth. At $g \approx 2h$, the additional bands appear in the spectrum.

The dependences of electron band boundaries on the tunneling-like level splitting Ω are shown in Fig. 7. Here, one can see the presence of two critical values $\Omega \approx 0.3$ (band splitting) and $\Omega \approx 0.6$ (band emerging).

The densities of states $\rho_\sigma(\omega) = \frac{1}{\pi} \mathrm{Im}\, G_\sigma^{(a)} \omega - i0^+)$ for different values of the pseudospin-electron interaction constant g are shown in Fig. 8. Initially, we observe the splitting of one band at $g \approx W$. Afterwards at $g \approx 2h$, two central bands emerge, and the further increase of g gives four bands in the electron spectrum.

7. Conclusions

1) The electron energy spectrum of the pseudospin-electron model is considered. For this purpose, the dynamical mean field method is applied. The effective single-site problem is solved within an original approach based on the use of a generalization of Wick's theorem. The alloy analogy approximation is used.

2) Electron transitions with a possibility of the simultaneous flip-over of the pseudospin (or at its unchanged orientation) manifest themselves in a complication of the electron spectrum which consists in the appearance of additional subbands. The effects of bond splitting and creation of new gaps take place, depending on the longitudinal field h, interaction constant g, and transverse field Ω values (Figs. 1–7).

3) The rearrangement of the spectrum, similarly to the Mott transition, occurs not only due to the on-site peudospin-electron interaction, but also under influence of the transverse field that intertangles the states with different pseudospin orientations.

4) The obtained results show that, in the real system, which exhibits the local anharmonicity of lattice vibrations, the metal-insulator transition due to the short-ranged electron correlation is influenced by the anharmonic subsystem. Changing the parameters of local anharmonicity (e.g., the potential well shape), one can affect the conditions of the appearance of a a gap.

5) The obtained results (Fig. 7) point out, in particular, that the additional gaps can appear in the fermion band spectrum at the increase of Ω. We have considered the case where, at $\Omega = 0$, the spectrum is already split. The problem in such a limit is reduced to the Falikov–Kimball model with a Mott gap at the chosen values of model parameters. In the case where PEM is applied to the boson-fermion mixtures on a lattice, the increase of the Ω parameter corresponds to the deepening into the phase with BE-condensate ($\Omega \sim \sum t_{ij}^{b} \langle S_j^x \rangle$). Additional gaps could appear at certain critical values of the order parameter $\langle S^x \rangle$. This problem (which now attracts an attention [21]) requires, however, a more detailed investigation. In the present study, based on the standard version of PEM, the boson transfer is taken into account in the mean field approximation. At the same time, the contributions of the collective pseudospin dynamics to the fermion spectrum can be essential.

6) It should be mentioned that we use an approach based on the formalism of X-operators. Such a scheme gives a possibility to consider, in a unified way, the creation of composite excitations (fermion+boson; fermion+boson hole) and their contributions to the total spectral density.

7) The more complete analysis of a reconstruction of the energy spectrum will be a subject of our subsequent consideration. It is referred, in particular, to the region of half-filling ($\mu \sim 0$, $h \sim \frac{g}{2}$), where the instability with respect to the appearance of a modulated (CDW-like) phase takes place in PEM at low enough temperatures. In such a case, the additional complication of the spectrum will arise as a result.

1. K.A. Müller, Z. Phys. B **80**, 193 (1990).
2. I.V. Stasyuk, in *Order, Disorder, and Criticality*, (World Sci., Singapore, 2007), vol. 2, p. 231.
3. T.S. Mysakovych, V.O. Krasnov, and I.V. Stasyuk, Ukr. J. Phys. **55**, 228 (2010).
4. G.D. Mahan, Phys. Rev. B **14**, 780 (1976).
5. I.V. Stasyuk and I.R. Dulepa, Cond. Matt. Phys. **10**, 259 (2007).
6. A. Albus, F. Illuminati, and J. Eisert, Phys. Rev. A **68**, 023606 (2003).
7. M. Lewenstein, L. Santos, M.A. Baranov, and H. Fehrmann, Phys. Rev. Lett. **92**, 050401 (2004).
8. M. Iskin and J.K. Freericks, Phys. Rev. A **80**, 053623 (2009).
9. A. Mering and M. Fleischhauer, Phys. Rev. A **83**, 063630 (2011).
10. F. Hébert, G.G. Batrouni, X. Roy, and V.G. Rousseau, Phys. Rev. B **78**, 184505 (2008).
11. T.S. Mysakovych, J. Phys. Stud.: Condens. Matter **22**, 355601 (2010).
12. W. Metzner and D. Vollhardt, Phys. Rev. Lett. **62**, 260 (1989).
13. W. Metzner, Phys. Rev. B 43, 8549 (1991).
14. E. Müller-Hartmann, Z. Phys. B **74**, 507 (1989).
15. I.V. Stasyuk and A.M. Shvaika, J. of Phys. Studies **2**, 177 (1999).
16. I.V Stasyuk, Cond. Matt. Phys. **3**, 437 (2000).
17. M. Potthoff, T. Herrmann, T. Wegner, and W. Nolting, Phys. Stat. Sol. (b) **210**, 199 (1998).
18. I.V. Stasyuk and A.M. Shvaika, Acta Phys. Polon. A **84**, 293 (1993).
19. I.V. Stasyuk and V.O. Krasnov, Cond. Matt. Phys. **9**, 725 (2006).
20. P.M. Slobodyan and I.V. Stasyuk, Theor. Math. Phys. USSR, **19**, 616 (1974).
21. E. Altman, E. Demler, and A. Rosch, Preprint arXiv:1205.4026v1, (2012).

І.В. Стасюк, В.О. Краснов

ЕНЕРГЕТИЧНИЙ СПЕКТР
ПСЕВДОСПІН-ЕЛЕКТРОННОЇ МОДЕЛІ
В МЕТОДІ ДИНАМІЧНОГО СЕРЕДНЬОГО ПОЛЯ

Р е з ю м е

Досліджено псевдоспін-електронну модель у випадку нескінченної взаємодії відштовхування електронів на вузлі. Електронний енергетичний спектр моделі розраховано в рамках методу динамічного середнього поля (ДСП) та наближення сплаву. Досліджено вплив псевдоспін-електронної взаємодії, локального поля асиметрії та тунельного розщеплення рівнів на існування та кількість електронних підзон. Обговорено можливість застосування псевдоспін-електронної моделі до розрахунку енергетичного спектра бозон-ферміонних сумішей в оптичних ґратках.